The viscous, viscoelastic and elastic characteristics of resting fast and slow mammalian (rat) muscle fibres

G. Mutungi and K. W. Ranatunga*

Department of Physiology, School of Medical Sciences, University of Bristol, Bristol BS8 1TD, UK

1. The tension and sarcomere length responses induced by ramp stretches (amplitude 1–3% of initial fibre length (L_0) and speeds of 0·01–12 L_0 s^{-1}) were examined, at 10 °C and sarcomere lengths of ~2·7 μm, in resting intact muscle fibre bundles isolated from the soleus (a slow muscle) and extensor digitorum longus (a fast muscle) of the rat.

2. In both fibre types, the tension response to moderately fast ramp stretches consists of a viscous, a viscoelastic and an elastic component. At low stretch velocities, where the viscous component is very small, the tension response consists of only the viscoelastic and elastic components.

3. The viscosity coefficient (mean ± S.E.M., 2 ± 0·01 kN s m^{-2}, $n = 12$) and the relaxation time of the viscoelasticity (44 ± 2 ms, $n = 12$) of the slow muscle fibres were significantly larger than those of the fast muscle fibres (0·8 ± 0·1 kN s m^{-2} and 11 ± 1 ms, respectively, $n = 20$).

4. The relaxation time, in either fibre type, is too long for the viscoelasticity to be due to rapidly cycling, weakly attached cross-bridges. Moreover, the tension components increased with sarcomere length and were insensitive to 5–10 mM 2,3-butanedione 2-monoxime (BDM), which inhibited active contractions.

5. The possibility that the fast–slow fibre differences may reflect differences in myoplasmic viscosity and connectin (titin) isoforms (in their gap filaments) is discussed.

In resting amphibian muscle or muscle fibre, the rising phase of the tension response to a ramp stretch shows a 'break' before the peak tension is reached at the end of the ramp. At low ramp stretch velocities, this break-point tension is relatively insensitive to stretching speed (Hill, 1968; Lannergren, 1971; Goldman & Simmons, 1986). Hill (1968) referred to this type of elasticity as short range elasticity (SRE) and attributed it to a small number of long-lived, slowly cycling cross-bridges. However, Lannergren (1971) found no evidence of cross-bridge involvement in SRE generation in both resting and submaximally activated single intact frog muscle fibres and attributed the SRE to a structural component within the filaments other than cross-bridges. At moderately high stretch velocities, on the other hand, the break-point tension is directly proportional to stretch velocity, indicating an apparent viscosity in resting muscle fibres (Ford, Huxley & Simmons, 1977; Bagni, Cecchi, Colomo & Garzella, 1995). The exact relation between these two 'break-point tensions' remains unclear, although Ford *et al.* (1977) suggested that they may have a common origin.

Detailed analyses of the rising phase of the tension response to moderately fast ramp stretches have shown that it consists of a viscous (P_1), a viscoelastic (P_2) and an elastic component (P_3) both in frog fibres (Bagni, Cecchi, Colomo & Garzella, 1992, 1995) and in mammalian (rat) fast fibres (Mutungi & Ranatunga, 1996*c*). The same tension components were present in the decay phase of the tension response and analyses of this phase revealed a 3- to 4-fold difference in the decay rates of the intermediate and slow components between fast and slow muscle fibres (Mutungi & Ranatunga, 1996*a*). The general proposal made in the above studies is that the viscoelasticity is not due to cycling cross-bridges but that it may reside in the gap (titin/connectin) filament and that the fibre type differences may reflect different titin isoforms. However, none of these studies employed very low stretch velocities to examine the SRE. Indeed, it is not clear whether SRE is present in mammalian muscle fibres and whether there may be fibre type (i.e. fast and slow) differences.

It is clear from the above that several issues regarding the mechanical properties of resting mammalian muscle fibres remain unresolved. The aim of the present study was firstly, to investigate the viscous and viscoelastic characteristics of resting, intact, mammalian (rat) muscle fibres (in particular, the slow fibres) and secondly, to compare the characteristics of fast and slow muscle fibres. Analysis of the tension

* To whom correspondence should be addressed.

response to ramp stretches (see Bagni *et al.* 1995) over a wide range of velocities shows that, functionally, there are only three tension components in either fibre type. Additionally, results show characteristic differences between fast and slow muscle fibres in their viscoelasticity.

Some data reported here were presented as abstracts to the European Muscle Conference (Mutungi & Ranatunga, 1996*b*) and to The Physiological Society (Mutungi & Ranatunga, 1995, 1996*d*).

METHODS

The materials and methods are as described by Mutungi & Ranatunga (1996*a*,*c*) and are only treated here briefly. Adult male rats (body weight, 213 ± 2·3 g) were killed with an overdose of sodium pentobarbitone (Sagatal; Rhône Mérieux Ltd, Harlow, Essex, UK) injected intraperitoneally and the soleus (a slow muscle) and extensor digitorum longus (a fast muscle) muscles carefully removed. Small bundles, containing up to ten muscle fibres were isolated under a dissecting microscope using dark-field illumination. Considerable care was taken in removing damaged fibres to ensure that those which extended from end to end in a bundle were intact and electrically excitable.

A preparation was mounted between two stainless steel hooks (one attached to a tension transducer and the other to a servomotor using aluminium foil clips): the details of the tension transducer and of the servomotor are described in Ranatunga (1994) and Mutungi & Ranatunga (1996*a*). The preparation was set up in a flow-through stainless steel chamber (volume, ~2 ml) that was mounted on an optical microscope assembly; the chamber was fitted with a glass window at the bottom and perfused (0·5 ml min^{-1}) with Ringer solution containing (mM): NaCl, 109; KCl, 5; $MgCl_2$, 1; $CaCl_2$, 4; $NaHCO_3$, 24; NaH_2PO_4, 1; sodium pyruvate, 10; and 200 mg l^{-1} of bovine fetal serum; the solution was continuously bubbled with 95% O_2 and 5% CO_2.

A fibre bundle was stimulated with single supramaximal stimuli at a rate of 1 per 60 s to 1 per 90 s, and small stretches were interposed between twitches during some cycles. The resting tension responses to ramp stretches of 100–300 μm amplitude (~1–3% of initial fibre length, L_0) completed in 0·5–1100 ms were examined at 10 °C. In addition the sarcomere length change in a 2 mm region of the bundle near the tension transducer was monitored using He–Ne laser diffraction (see Mutungi & Ranatunga, 1996*a*,*c*). The temperature control (± 0·1 °C) was achieved by means of a Peltier device fitted underneath the muscle chamber and it was monitored with a thermocouple placed inside the muscle chamber.

Data recording and analyses

The length signal (from the motor), the sarcomere length signal (from the diffractometer) and the tension transducer signal were collected via a CED 1401 laboratory interface using Signal Averager software (Cambridge Electronic Design Ltd, Cambridge, UK) and stored in a Tandon computer (Target 386SX-40); up to ten responses were averaged at low stretch velocities in order to increase the signal-to-noise ratio. Additionally, the tension transducer output and the thermocouple output were continuously recorded on a chart recorder. Initial analyses of the tension response for estimating the peak tension, the steady tension after relaxation (P_3) and the tension at the 'break-points' (P_1 and/or 'apparent break-point') were made using the Signal Averager software; a 'break-point tension' was determined as the tension at the point of intersection between two linear slopes (fitted to the rising phase on either side of the break). For convenient description, the break on the rising phase of tension responses at low velocities will be referred to as an 'apparent break-point', whereas the sharp initial break (P_1) seen at higher velocities will be referred to as a 'break-point'. Further analyses of the data, involving curve fitting to P_2 data, subtraction of P_3, etc., were done using Fig.P software (Biosoft). The equation fitted to P_2 *versus* reciprocal stretch duration was:

$$P_2 = lkt_r/t_d(1 - \exp(-t_d/t_r)),$$

where l is stretch amplitude, k is stiffness, t_r is relaxation time and t_d is stretch duration (see Bagni *et al.* 1995). Since the ramp stretch amplitude was constant in a given series, $1/t_d$ was directly proportional to stretch velocity and a similar equation could be used for P_2 *versus* stretch velocity plots (see Fig. 6); the sum of such a P_2 *versus* velocity curve and the linear regression of P_1 *versus* velocity (and a constant, P_3) could fit the peak tension (PT) *versus* stretch velocity data (Fig. 3*A*). The data reported here were obtained from muscle fibre bundles held at an initial sarcomere length (SL_0) of 2·6–2·8 μm unless otherwise stated.

RESULTS

General features of the tension responses

Figure 1*A* and *B* shows at two different time scales the same tension (upper) and sarcomere length (lower) responses recorded from a soleus preparation when a moderately fast (~3 L_0 s^{-1}) ramp stretch (middle trace) was applied. The tension response was qualitatively similar to that reported in single intact frog muscle fibres (Bagni *et al.* 1995) and in intact rat fast muscle fibre bundles (Mutungi & Ranatunga, 1996*c*). During the stretch, the tension rose rapidly to reach a peak (PT) at the end of the ramp; thereafter, the tension decayed in a complex manner to a plateau tension (P_3) at the stretched length when the sarcomere length was relatively constant (Fig. 1*A*). Figure 1*B* shows the first ~30 ms of the same tension record (continuous line); the rising phase consisted of an initial rapid rise to a 'break' (P_1) followed by a slower tension rise (an apparent P_2). Figure 1*B* also illustrates further analysis; the dotted line is the sarcomere length record (with its amplitude normalized to the steady P_3 tension measured after a long interval) representing the P_3 tension response (assuming that P_3 tension is elastic (see Fig. 3) and therefore changes in the same way as the sarcomere length) and the dashed line is the difference tension trace obtained by subtracting the P_3 component from the original tension trace. The rising phase of the difference trace itself shows two components, an initial fast rise (P_1; arrowhead) followed by a slow rise (net P_2). Figure 1*C* shows a tension record (continuous line) obtained using a low stretching speed (~0·1 L_0 s^{-1}); the tension response shows an 'apparent break' on the rising phase (asterisk). P_1 amplitude (being viscous tension, see Figs 2 and 3) was relatively small at this low velocity. Therefore, subtracting the P_3 component (as in Fig. 1*B*) from the tension response leaves only a single component (dashed line) displaying characteristics of a viscoelasticity (P_2). In their careful study on single frog fibres, Bagni *et al.* (1992,

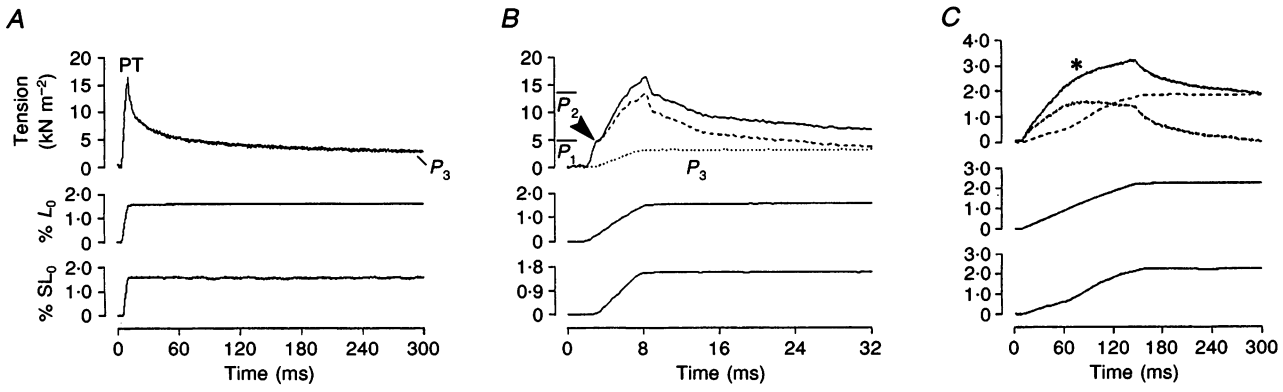

Figure 1. General features of the tension response to a ramp stretch

The tension response (upper trace) and the sarcomere length response (as % SL_0; lower trace) induced by a moderately rapid ramp stretch (% L_0; middle trace) are displayed at two different time scales in *A* and *B*. The dotted line in *B* is the sarcomere length record with its amplitude normalized to P_3 tension, and it represents the net P_3 tension response. Subtracting the P_3 tension trace from the original tension response gave the difference trace (dashed line), which in this case consists of P_1 and P_2 tension components, separated by a break (arrowhead). *C* shows records and similar analyses on a tension response to a slow ramp stretch. The difference trace consists of only a viscoelastic component (P_2): a sharp initial break corresponding to P_1 is absent and, for convenient identification, the point at which the slope of the rising phase gradually decreases (asterisk) will be referred to as an 'apparent break-point'.

1995) showed that the break-point on the rising phase was precisely coincident with the onset of the constant velocity phase in the sarcomere length record; to some extent, this was evident in our records with respect to either break-point.

The analysis in Fig. 1*B* and *C* indicates that the tension response at a moderately high stretch speed may be resolved into three components (P_1, P_2 and P_3) whereas that at a low speed contained only two components (P_2 and P_3). Therefore, the 'apparent break' seen on the rising phase of the tension record at low stretch speed (asterisk, Fig. 1*C*) and the 'break' seen at the higher speed (Fig. 1*B*) have a different underlying basis.

Figure 2 shows tension (upper) and sarcomere length (lower) records from a soleus bundle; as the different time scales indicate, the records are responses at three different stretch speeds (> 0·5 L_0 s^{-1}) where an initial 'break' was clearly seen on the original tension record (P_1, arrowhead). The records show that peak tension and P_1 amplitude increased significantly with the stretch speed.

The way the various tension components vary with stretch velocity is shown from the complete analysis in Fig. 3; the data are from a single soleus preparation. The break-point tension (P_1), the peak tension (PT) and the plateau tension (P_3, measured at 300 ms or more after the stretch) were measured and the net P_2 tension was calculated by

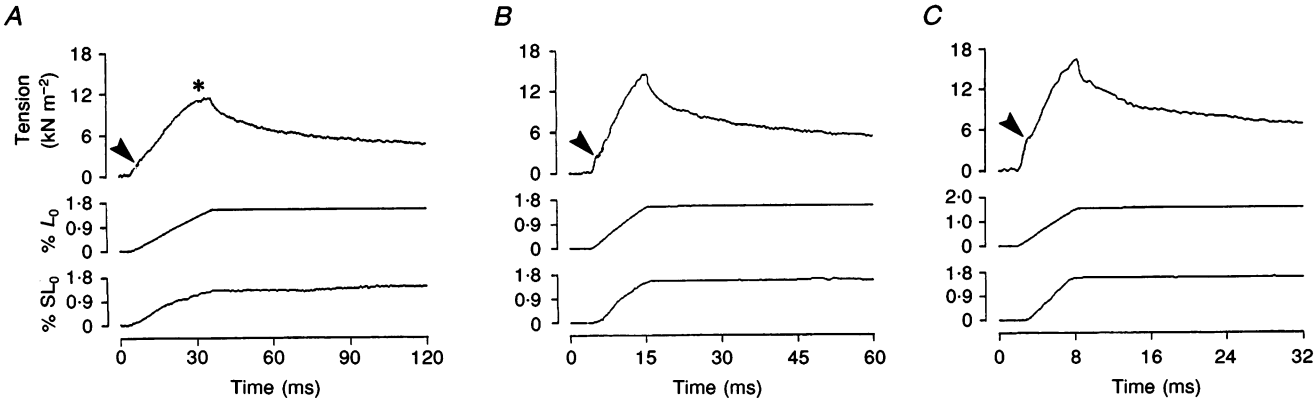

Figure 2. Dependence on stretch velocity

Tension (upper trace) and sarcomere length (lower trace) records from a slow muscle fibre bundle subjected to ramp stretches (middle trace) at three different speeds are shown in *A*, *B* and *C*; the amplitudes of P_1 tension (arrowheads) and peak tension increase with stretch speed. Note that two break-points, one corresponding to P_1 (arrowhead) and the other to the 'apparent break' (asterisk), can be seen in *A*.

subtracting $P_1 + P_3$ tensions from the peak tension. In Fig. 3*A* the peak tension (circles) and the P_3 tension (triangles) are plotted against stretch velocity. As in fast fibres (Mutungi & Ranatunga, 1996*a*), the peak tension increased with stretch velocity, while P_3 tension was relatively independent of stretch velocity (suggesting that P_3 has characteristics of an elastic tension).

The break-point tension (P_1) is plotted against stretch velocity in Fig. 3*B* and it can be seen that P_1 tension increased in direct proportion to stretch velocity (viscous). The fitted line is the calculated linear regression for the data, the slope of which corresponds to a viscosity coefficient of 2·4 kN s m^{-2} (per L_0). Net P_2 amplitude is plotted against reciprocal stretch duration (see Bagni *et al.* 1995) in Fig. 3*C*; since stretch amplitude was constant, the reciprocal stretch duration was directly proportional to stretch velocity and it is seen that P_2 increased with velocity up to a plateau (it was viscoelastic, i.e. a viscous element in series with an elastic element). Analysis of the P_2 tension data by curve fitting (see figure legend), as described by Bagni *et al.* (1995), gave a relaxation time of 40 ms. (The reason why the P_2 tension is decreased at very high velocities remains unclear; this was observed in several slow fibre preparations, but not in fast fibre preparations.)

As previously reported in fast muscle fibres (see Mutungi & Ranatunga, 1996*c*), the addition of 5–10 mM 2,3-butanedione 2-monoxime (BDM; which almost abolished active twitch tension) had no effects on the various tension

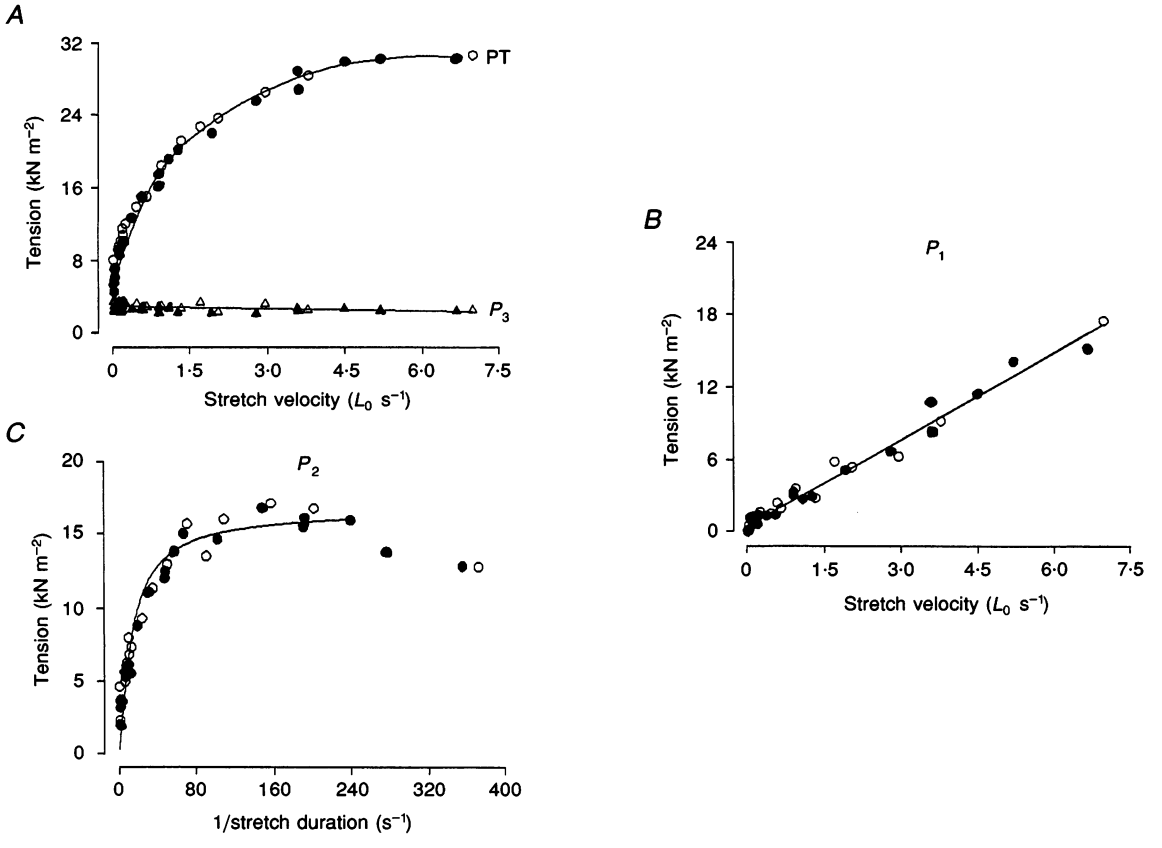

Figure 3. Analyses of tension components

Data are from a slow muscle fibre preparation illustrating the velocity dependence of the amplitude of the various tension components. In *A*, peak tension (PT) and P_3 tension are plotted against stretch velocity; PT increases (to a plateau) with stretch velocity (curve fitted is the sum of P_2 curve against stretch velocity, P_1 curve and a residual; see Methods), but P_3 remains relatively constant (the line fitted is the calculated linear regression; $P > 0{\cdot}1$). *B* shows P_1 tension plotted against stretch velocity; P_1 tension increases in direct proportion to stretch velocity and the slope calculated from the fitted regression line ($P < 0{\cdot}001$) corresponds to a viscosity coefficient of 2·4 kN m^{-2}/L_0 s^{-1}. *C* shows P_2 tensions (calculated as PT minus ($P_1 + P_3$)) plotted against reciprocal stretch duration, as suggested by Schoenberg (1988) for analysis of viscoelasticity; the reason why P_2 tension data are lower at high velocities (high reciprocal stretch durations) remains uncertain. The curve represents the equation used by Bagni *et al.* (1995) fitted to the data; the relaxation time is 40·3 ms and the plateau tension normalized to length change (i.e. as Young's modulus) is 950 kN m^{-2}. The open symbols represent data obtained in the presence of 10 mM 2,3-butanedione 2-monoxime (BDM) and the filled symbols show data obtained without added BDM (i.e. in normal Ringer solution, before and after the exposure to BDM-containing Ringer solution); the addition of 10 mM BDM had no effect on the characteristics of the various tension components.

components (open symbols in Fig. 3). In addition, the various tension components were larger at longer initial sarcomere lengths; this is shown by the data from one preparation illustrated in Fig. 4.

Responses at low stretch speed: 'short range elasticity'?

The analyses presented so far were based on measurements of peak tension, steady tension after tension relaxation (P_3) and the tension value at the initial 'break-point' (P_1) in slow muscle fibres; the residual tension was taken as the P_2 component, but no account was taken of the 'apparent break-point' tension seen particularly at low velocities (Fig. 1*C*). With a stretch amplitude of ~2% L_0, evidence of an 'apparent break' was seen at speeds of up to ~2 L_0 s^{-1} in both fast and slow muscle fibre types, and the occurrence of two 'breaks' on the rising phase was clear at certain intermediate stretch speeds. This is illustrated in Fig. 5, which shows the tension response (upper trace) and the sarcomere length record (lower trace) from a slow (*A–C*) and a fast (*D–F*) muscle preparation at three different ramp stretch velocities (record not shown). When examined at appropriate time scales, the initial 'break-point' (P_1) was clear in *B*, *C*, *E* and *F* and is indicated by an arrowhead, and the 'apparent break' is shown by an asterisk. Superimposed on each tension response (dotted trace) is the difference tension curve obtained as in Fig. 1*B* and *C*. From these results it can be seen that the difference tension curve (largely due to P_2, see below) is more prominent and present at all stretch speeds in the slow fibre. However, it almost disappears at very slow stretch speeds in fast muscle fibres and at these speeds, the tension response consists mainly of the elastic (P_3) tension (see Fig. 5*D*).

In the original experiments of Hill (1968) and in the subsequent studies by Lannergren (1971) and Goldman & Simmons (1986) the tension at the (apparent) break-point was measured at different stretch velocities. Since our tension records at low stretch speeds bear a striking similarity to those reported by Hill (1968) from frog muscle, we carried out similar analyses in a number of experiments; the data shown in Fig. 6 illustrate typical findings from a slow (*A*) and a fast (*B*) fibre bundle. The amplitude of the 'apparent' break-point (▲) did not increase linearly with stretch velocity (not viscous), contrasting with the behaviour of P_1 (●). The length at which the apparent break in the rate of tension rise occurred was also measured in previous studies, as the elastic limit of SRE (this was ~0·2–0·4% of L_0 in frog muscle). In our experiments on rat muscle, and at these low velocities, the elastic limit of the apparent break increased with stretch velocity in both fibre types and it was 3–4 times longer in slow than in fast muscle fibres.

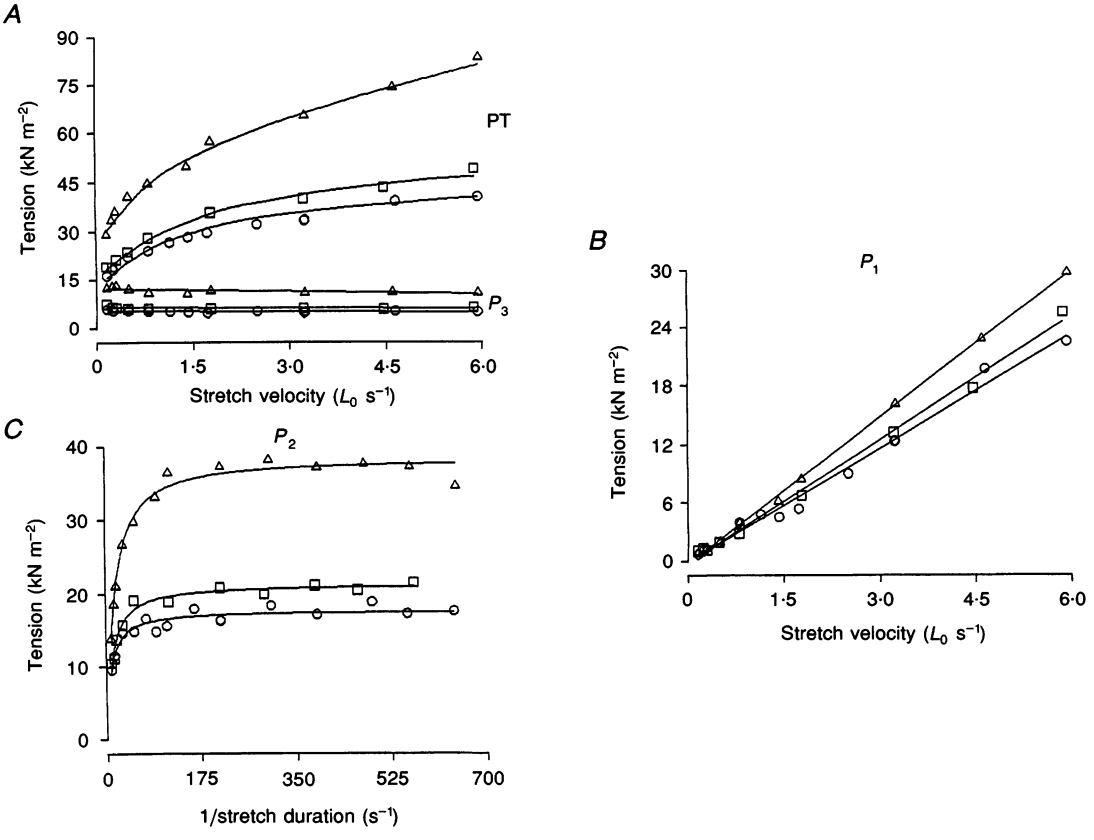

Figure 4. Effects of initial sarcomere length

The data are from one slow fibre bundle held at three different initial sarcomere lengths of 2·5 μm (○), 2·71 μm (□) and 3·07 μm (△); data presentation is similar to Fig. 3. Note that the amplitudes of all the component tensions are higher at longer sarcomere length.

It is pertinent to note that the tension rise to the 'apparent break' had a characteristic time course; moreover, the rise time was longer in slow than in fast fibres (see Fig. 5), and the difference was about the same as that found for the relaxation time of the P_2 component (see below). Additionally, if the analysis performed and displayed in Fig. 3 is carried out, the tension responses at low velocities can also be resolved into individual P_1 and P_2 (and P_3) components. Data from two different preparations are shown in Fig. 6; the circles show P_1 and P_2 values (the curves were fitted as previously) and the triangles show the measured tension values at the 'apparent break-point'. The dashed lines in Fig. 6*A* and *B* show the expected 'apparent break-point' tension level obtained by assuming that the tension at this point was the sum of the individual tension components (P_1, P_2 and P_3). P_1 and P_2 tensions were obtained from the fitted curves (shown in Fig. 6) while the component of P_3 tension added to it was obtained from the P_3 tension curve (from the sarcomere length response normalized to steady P_3 tension) at the appropriate time interval. It is evident that the dashed lines fit well to the measured values of 'apparent break-point' (▲) at low velocities but deviate at higher speeds. The discrepancy was particularly marked in the fast fibre. This could be due to the fact that the 'apparent break-point' was not well defined at these higher velocities (the discrepancy was not much reduced even when the 'apparent break-point' was estimated as the point of intersection of the two linear slopes). On that basis, the 'apparent break' on the rising phase is due to the viscoelastic behaviour of the P_2 component; the stretch amplitude being the same, the P_2 component was expected to be more prominent at lower stretch speeds simply due to the longer stretch duration coupled with the smaller, and hence less marked, P_1 component.

Comparison between fast and slow muscle fibres

Figure 7 compares, in the form of scatter plots, the data for various measurements from twelve slow fibre bundles and twenty fast fibre bundles (fast fibre data include the data

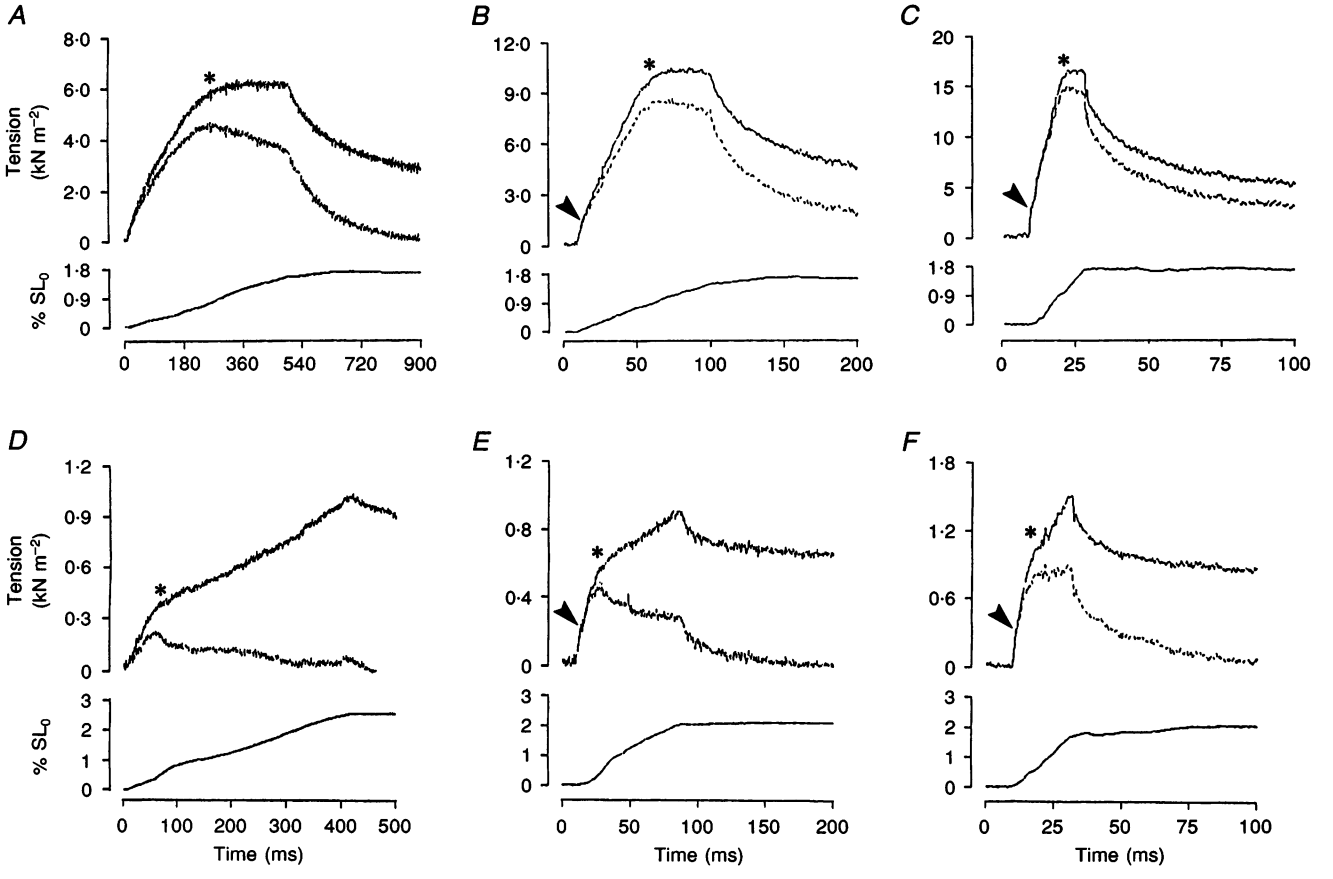

Figure 5. Tension responses at low stretch speeds

Tension (top trace) and sarcomere length (bottom trace) responses to slow ramp stretches (not shown) from a slow (*A–C*) and a fast (*D–F*) muscle fibre bundle are shown. The initial break-point (P_1) on the rising phase of a tension response is labelled with an arrowhead and the 'apparent break-point' with an asterisk. The dotted (middle) trace in each frame is the difference tension trace obtained by subtracting the P_3 tension record from the original tension response (as in Fig. 1*B* and *C*). Note that the net P_2 component is present at all stretch speeds in slow fibres but is almost absent in fast muscle fibres at the lowest speed (*D*). P_1 tension becomes apparent only at higher stretch speeds in both fibre types (*B*, *C*, *E* and *F*), where two break-points are seen.

from Mutungi & Ranatunga, 1996*a*). The average fibre lengths (L_0) in the preparations ranged from 9 to 14·5 mm (mean ± S.E.M., 11·2 ± 0·4 mm) in the fast muscle fibre bundles and from 11 to 15 mm (13·4 ± 0·4 mm) in the slow ones and their cross-sectional areas showed considerable overlap. Figure 7*A* shows the viscosity coefficient data (from P_1 analyses, see Fig. 3*B*) and Fig. 7*B* shows the P_3 tension data (normalized to stretch amplitude, i.e. as Young's modulus), both plotted against cross-sectional area. Despite the large scatter, the difference between the two fibre types is evident. Corresponding plots for P_2 plateau tension (as Young's modulus) and P_2 relaxation time are given in Fig. 7*C* and *D*, respectively; the plateau P_2 tension is 5–10 times larger and the relaxation time ~4 times longer in the slow fibres. The difference in the relaxation times remained at different sarcomere lengths (not illustrated).

DISCUSSION

The tension response to a ramp stretch over a wide range of stretch velocities, and in both fast and slow fibres, consists of only three components – a viscous, a viscoelastic and an elastic component. Since the same stretch amplitude was used in a given series, the viscous component is prominent at high velocities and is noticeable as a 'break' on the rising phase. On the other hand, due to longer stretch duration and a smaller viscous component, the viscoelastic component becomes more prominent at the low velocities and its behaviour provides the 'apparent break' on the rising phase. As stated in the Results section (Figs 3 and 4) and reported before for frog (Bagni *et al.* 1995) and for fast mammalian muscle fibres (Mutungi & Ranatunga, 1996*c*), there is no evidence that cycling cross-bridges underlie any of the components. Thus, the tension components became larger with decreased filament overlap (at longer sarcomere length) and were insensitive to 5–10 mM BDM. Moreover, the relaxation time in both fibre types is too long (> 1 ms) for the viscoelasticity to be due to rapidly cycling, weakly attached cross-bridges as suggested by Brenner, Schoenberg, Chalovich, Greene & Eisenberg (1982) and Schoenberg (1988) using skinned rabbit psoas muscle fibres at 4 °C and low ionic strength. Also, it should be clear from the results that the tension responses to slow stretches showed no evidence of a short range elasticity (SRE) with a constant elastic limit of 0·2–0·4% (and hence no evidence of slowly cycling cross-bridges) as described for frog muscle (Hill, 1968). From the analyses we presented, the tension component that becomes prominent at low stretch velocities is the viscoelastic, P_2, component (see Figs 5 and 6).

The characteristics of the various tension components showed significant quantitative differences between fast and slow muscle fibres. For example, the viscosity coefficient derived from analysis of the initial break-point tension (P_1) is ~2 times larger in slow fibres. It is important to note that the viscous tension (P_1) is considerably reduced after skinning in frog fibres (Bagni *et al.* 1995) and such a reduction may result from swelling of the myofilament lattice (Goldman &

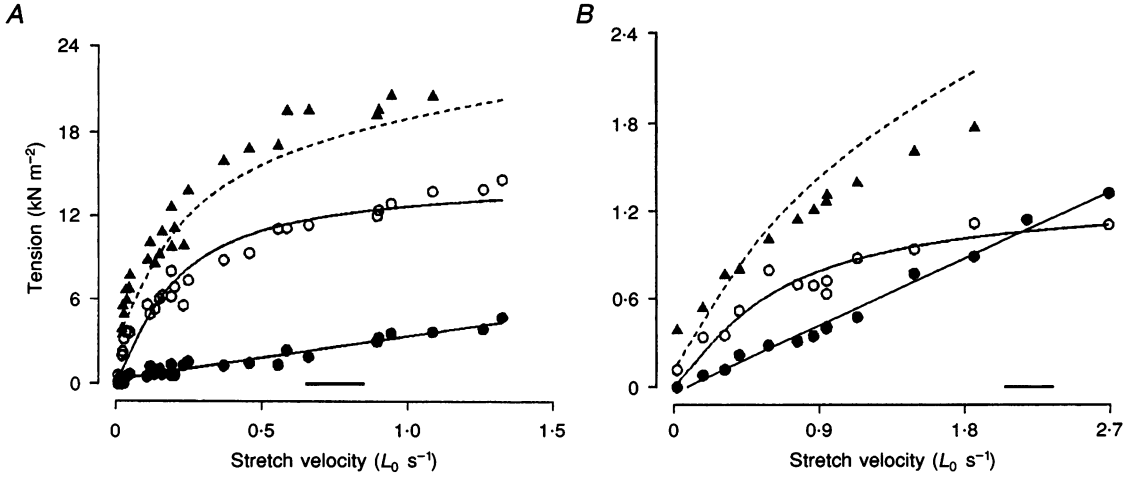

Figure 6. Analysis of 'apparent break-point' tension (low stretch speed)

Triangles show the measured tension values at the 'apparent break-point' from a slow (*A*) and a fast (*B*) muscle fibre bundle (subjected to slow ramp stretches), plotted against stretch velocity; the 'apparent break-point' tension increases with stretch velocity in both fibre types. Additionally, P_1 tension (●) and net P_2 tension (○) obtained from the same records are also plotted and analysed. The dashed line represents the calculated tension for the 'apparent break-point'; it was calculated as the sum of P_1, P_2 and a component of P_3 tension (the P_3 tension value at the appropriate time interval was determined using the normalized sarcomere length record and the time to 'apparent break-point'). There is a fair correspondence between the measured tension values for 'apparent break-point' and the calculated curve for slow muscle. The horizontal bar indicates the maximum shortening velocity range (mean ± S.E.M.) of the two muscles at 10 °C (data from Ranatunga, 1984).

Simmons, 1986) and decreased myoplasmic viscosity in the skinned fibres. Thus, P_1 may arise from the inter-filamentary viscous resistance to stretch within sarcomeres, as suggested by Bagni *et al.* (1992). On that basis, and assuming that the sarcomeric ultrastructure and dimensions are similar between fast and slow mammalian fibres, the difference in the viscosity coefficient reflects a higher myoplasmic viscosity in slow fibres than in fast fibres. Mammalian slow ('red') fibres contain ~4 times more myoglobin (Dawson & Romanul, 1964) and ~20% more glycogen (Gillespie, Simpson & Edgerton, 1970) than fast ('white') fibres; however, the amounts involved (2–3 mg g^{-1} more in slow fibres) seem too small to result in a significantly higher myoplasmic viscosity in the slow fibres. Compared with fast fibres, mammalian slow fibres have a higher mitochondrial volume, a higher lipid droplet volume and a wider Z-membrane in their sarcomeres (see Padykula & Gauthier, 1967; Eisenberg, 1974); the significance of such differences to the present findings is unclear.

The results show that the viscosity coefficients for intact rat fibres at a sarcomere length of 2·7 μm and at 10 °C are ~0·8–2 kN s m^{-2}; the values would be smaller (~0·5–1·5 kN s m^{-2}) at a resting sarcomere length of ~2·5 μm (see Mutungi & Ranatunga, 1996*c*). Thus, at maximum shortening velocities of 2·2 L_0 s^{-1} in the fast fibres and 0·75 L_0 s^{-1} in the slow fibres at 10 °C (see Fig. 6 and Ranatunga, 1984), the viscous resistance would be ~1 kN m^{-2} in both fibre types, which is < 1% of the maximum tetanic tension. The viscosity coefficients for rat fibres are some 10–30 times larger than those reported for intact frog fibres at 15 °C (~0·05 kN s m^{-2}; Bagni *et al.* 1995). Ford *et al.* (1977) obtained viscosity coefficients of $1{\cdot}5 \times 10^8$ to 4×10^8 N s m^{-3} for half-sarcomere in frog fibres at 0–3 °C; interestingly, corresponding calculation for rat fast fibres gives a similar value (~4×10^8 N s m^{-3}). The above considerations show that the viscous resistance in resting intact muscle fibres varies considerably depending on species, fibre types, sarcomere length and temperature.

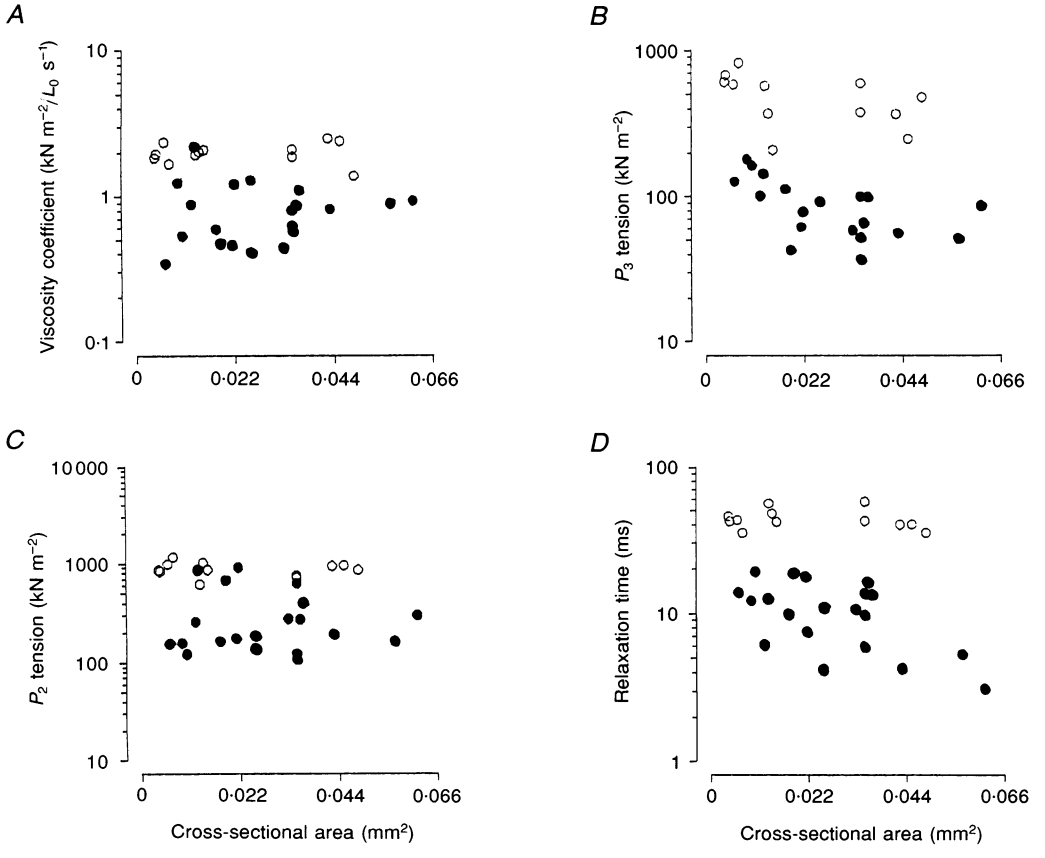

Figure 7. Fast and slow muscle fibre comparison

Pooled data for viscosity coefficient (*A*), P_3 tension (*B*), P_2 plateau tension (*C*) and relaxation time (*D*) obtained from twelve slow fibre bundles (○) and twenty fast fibre bundles (●) at a sarcomere length of 2·7 μm and at 10 °C are plotted against fibre cross-sectional area; both P_2 and P_3 tensions are normalized to length change (i.e. represent Young's moduli). Except for P_3 tension in fast muscle fibres all the other values showed no correlation to fibre cross-sectional area. Fibre length and cross-sectional area were not significantly different ($P > 0{\cdot}05$), but all the other parameters were significantly different ($P < 0{\cdot}001$) between the two fibre types.

The plateau tension of the viscoelastic component (P_2, normalized to stretch amplitude) is some 5-fold larger and its relaxation time ~4-fold longer in slow fibres than in fast fibres. Values for both measurements in slow fibres and for relaxation time in fast fibres are larger than those reported for frog fibres (normalized plateau tension of 100–700 kN m^{-2} and a relaxation time of ~1 ms; Bagni *et al.* 1995). Although cross-bridge involvement is ruled out (see above), the exact structural basis of the P_2 component and its differences remain uncertain. The fact that our data from intact fibre bundles are basically similar to those reported by Bagni *et al.* (1995) from single (intact and skinned) muscle fibres of the frog indicates that the viscoelasticity resides within muscle fibres. It may arise from the cytoskeleton as proposed by Bagni *et al.* (1995) and/or from within the sarcomeric ultrastructure itself. De Tombe & ter Keurs (1992) indeed proposed that the viscoelasticity in cardiac sarcomeres originates from the titin (connectin)-containing gap filament.

Data obtained using gel electrophoresis (Hu, Kimura & Maruyama, 1986; Horowits, 1992) and monoclonal antibody reactivity tests (Hill & Weber, 1986) have revealed the presence of different titin isoforms in different striated muscle fibre types. Moreover, the expression of different titin isoforms in the various fibre types is thought to control and modulate their resting stiffness and elasticity (Wang, McCarter, Wright, Beverly & Ramirez-Mitchell, 1991; Horowits, 1992). It is, therefore, conceivable that the viscoelasticity reflects properties of the gap filament + thick filament complex and the fast–slow differences are due to different titin (connectin) isoforms in the gap filaments. It is now clear that only a segment of the I-band part of titin is extensible (Labeit & Kolmerer, 1995; Granzier, Helmes & Trombitas, 1996) and that the length of the extensible part may be different in the various fibre types; the mechanism of titin 'elasticity', however, remains unclear (see Politou, Thomas & Pastore, 1995). If our interpretation is correct, then titin 'elasticity' should be visualized as more 'complex' and 'viscoelastic' rather than as 'simple elastic'.

Irrespective of the exact structural basis of the viscoelasticity, it is interesting to note that the difference seen between the relaxation time of the viscoelastic component of slow muscle fibres and that of fast fibres is similar to the differences previously reported in their active contraction speeds (e.g. shortening velocity and rate of tension development; see Ranatunga, 1984). Indeed, a similar difference was observed in our analyses of the resting tension relaxation after stretch (Mutungi & Ranatunga, 1996*a*) and as suggested in that paper, such fibre type-specific differences seem to imply that passive viscoelasticity and active cross-bridge cycling are closely matched. A coupling of this nature may ensure the efficient transfer of power during active muscle contraction especially during muscle fibre shortening or lengthening.

In conclusion, our data show that the passive viscoelastic characteristics of intact rat fibre bundles at 10 °C are basically similar to those reported from single frog fibres. However, there are quantitative differences between rat fast and slow fibres. It would be particularly important to know whether such differences exist at the level of myofibrils and how they change in warming to physiological temperatures (> 30 °C).

Bagni, M. A., Cecchi, G., Colomo, F. & Garzella, P. (1992). Are weakly binding bridges present in intact muscle fibers? *Biophysical Journal* **63**, 1412–1415.

Bagni, M. A., Cecchi, G., Colomo, F. & Garzella, P. (1995). Absence of mechanical evidence for attached weakly binding cross-bridges in frog relaxed muscle fibres. *Journal of Physiology* **482**, 391–400.

Brenner, B., Schoenberg, M., Chalovich, J. M., Greene, L. E. & Eisenberg, E. (1982). Evidence for crossbridge attachment in relaxed muscle at low ionic strength. *Proceedings of the National Academy of Sciences of the USA* **79**, 7288–7291.

Dawson, D. M. & Romanul, F. C. A. (1964). Enzymes in muscle. II. Histochemical and quantitative studies. *Archives of Neurology* **11**, 369–377.

de Tombe, P. P. & ter Keurs, H. E. D. J. (1992). An internal viscous element limits unloaded velocity of sarcomere shortening in rat myocardium. *Journal of Physiology* **454**, 619–642.

Eisenberg, B. R. (1974). Quantitative ultrastructural analysis of adult mammalian skeletal muscle fibers. In *Exploratory Concepts in Muscular Dystrophy II*, ed. Milhorat, A. T., pp. 258–270. Excerpta Medica, Amsterdam.

Ford, L. E., Huxley, A. F. & Simmons, R. M. (1977). Tension responses to sudden length change in stimulated muscle fibres at near slack length. *Journal of Physiology* **269**, 441–515.

Gillespie, C. A., Simpson, D. R. & Edgerton, V. R. (1970). High glycogen content of red as opposed to white skeletal muscle fibers of guinea pigs. *Journal of Histochemistry and Cytochemistry* **18**, 552–558.

Goldman, Y. E. & Simmons, R. M. (1986). The stiffness of frog skinned muscle fibres at altered lateral filament spacing. *Journal of Physiology* **378**, 175–194.

Granzier, H., Helmes, M. & Trombitas, K. (1996). Nonuniform elasticity of titin in cardiac myocytes: A study using immunoelectron microscopy and cellular mechanics. *Biophysical Journal* **70**, 430–442.

Hill, C. & Weber, K. (1986). Monoclonal antibodies distinguish titins from heart and skeletal muscle. *Journal of Cell Biology* **102**, 1099–1108.

Hill, D. K. (1968). Tension due to interaction between the sliding filaments in resting striated muscle. The effect of stimulation. *Journal of Physiology* **199**, 637–684.

Horowits, R. (1992). Passive force generation and titin isoforms in mammalian skeletal muscle. *Biophysical Journal* **61**, 392–398.

Hu, D., Kimura, S. & Maruyama, K. (1986). Sodium dodecyl sulfate gel electrophoresis studies of connectin-like high molecular proteins of various vertebrate and invertebrate muscles. *Journal of Biochemistry* **104**, 504–508.

Labeit, S. & Kolmerer, B. (1995). Titins: Giant proteins in charge of muscle ultrastructure and elasticity. *Science* **270**, 293–296.

LANNERGREN, J. (1971). The effect of low level activation on the mechanical properties of isolated frog muscle fibres. *Journal of General Physiology* **58**, 145–162.

MUTUNGI, G. & RANATUNGA, K. W. (1995). Tension responses to ramp stretch in intact slow twitch rat muscle fibres. *Journal of Physiology* **483.P**, 80*P*.

MUTUNGI, G. & RANATUNGA, K. W. (1996*a*). The tension relaxation after stretch in resting mammalian muscle fibers: Stretch activation at physiological temperatures. *Biophysical Journal* **70**, 1432–1438.

MUTUNGI, G. & RANATUNGA, K. W. (1996*b*). Visco-elasticity of relaxed, intact, mammalian (rat) slow muscle fibres. *Journal of Muscle Research and Cell Motility* **17**, 122.

MUTUNGI, G. & RANATUNGA, K. W. (1996*c*). The visco-elasticity of resting intact mammalian (rat) fast muscle fibres. *Journal of Muscle Research and Cell Motility* **17**, 357–364.

MUTUNGI, G. & RANATUNGA, K. W. (1996*d*). Characteristics of the short range elasticity (SRE) in mammalian (rat) muscle fibres. *Journal of Physiology* **493.P**, 7–8*P*.

PADYKULA, H. H. & GAUTHIER, G. F. (1967). Morphological and cytochemical characteristics of fiber types in normal mammalian skeletal muscle. In *Exploratory Concepts in Muscular Dystrophy and Related Disorders*, ed. MILHORAT, A. T., pp. 117–131. Excerpta Medica Foundation, Amsterdam.

POLITOU, A. S., THOMAS, D. J. & PASTORE, A. (1995). The folding and stability of the titin immunoglobulin-like modules, with implications for the mechanism of elasticity. *Biophysical Journal* **69**, 2601–2610.

RANATUNGA, K. W. (1984). The force–velocity relation of rat fast- and slow-twitch muscles examined at different temperatures. *Journal of Physiology* **351**, 517–529.

RANATUNGA, K. W. (1994). Thermal stress and Ca-independent contractile activation in mammalian skeletal muscle fibers at high temperatures. *Biophysical Journal* **66**, 1531–1541.

SCHOENBERG, M. (1988). Characterization of the myosin adenosine triphosphate (M.ATP) crossbridge in rabbit and frog skeletal muscle fibers. *Biophysical Journal* **54**, 135–148.

WANG, K., MCCARTER, R., WRIGHT, J., BEVERLY, J. & RAMIREZ-MITCHELL, R. (1991). The regulation of skeletal muscle stiffness and elasticity by titin isoforms: A test of the segmental extension model of resting tension. *Proceedings of the National Academy of Sciences of the USA* **88**, 7101–7105.

Acknowledgements

We thank The Wellcome Trust for support.

Author's email address

K. W. Ranatunga: K.W.Ranatunga@Bristol.ac.uk

Received 12 March 1996; accepted 17 July 1996.